Int. J. Heat Mass Transfer. Vol. 24, No. 7, pp. 1267–1276, 1981
Printed in Great Britain

0017-9310/81/071267-10 $02.00/0
Pergamon Press Ltd.

CRITICAL HEAT FLUX AND EXIT FILM FLOW RATE IN A FLOW BOILING SYSTEM

TATSUHIRO UEDA and YASUSHI ISAYAMA
Department of Mechanical Engineering, University of Tokyo, Bunkyo-ku, Tokyo, Japan

(*Received* 20 *August* 1980)

Abstract—Critical heat flux and liquid film flow rate at exit end of the test tube are measured with Freon 113 upward flow in a uniformly heated tube. The exit film flow rate at the critical heat flux condition is near to zero in all cases of the exit qualities higher than 50%, however, the exit film flow rate tends to increase as the heat flux is increased and the exit quality decreases less than 50%. A correlation is proposed for the critical condition with high heat fluxes, suggesting that the liquid film separation from the heated surface by vapor generation takes an important part of the critical phenomenon.

NOMENCLATURE

C,	droplet concentration;
D,	tube diameter;
G,	mass velocity;
h_{fg},	heat of vaporization;
h_{TP},	heat transfer coefficient;
K,	droplet deposition coefficient;
L,	heating length;
L_s,	boiling length;
M_f,	liquid film flow rate;
p,	pressure;
q,	heat flux;
T,	temperature;
u,	liquid velocity;
u_m,	mean velocity of liquid film at exit end of heating section;
x,	quality;
y_l,	liquid film thickness;
y_l^+,	non-dimensional film thickness;
z,	tube length.

Greek symbols

Γ,	liquid film flow rate per unit periphery, $\Gamma = M_f/\pi D$;
μ_g,	vapor viscosity;
μ_l,	liquid viscosity, $\mu_l = \rho_l \nu_l$;
ρ_g,	vapor density;
ρ_l,	liquid density;
σ,	surface tension;
τ,	shear stress;
Φ_G, X_{tt},	Lockhart–Martinelli parameters.

Subscripts

c,	critical heat flux condition;
ex,	exit end of heating section;
in,	inlet end of heating section;
s,	saturation condition;
w,	wall surface.

1. INTRODUCTION

THE CRITICAL heat flux in flow boiling systems gives a most important design boundary in such high performance heat exchangers as steam generators and nuclear reactors. A great deal of work has been made on this problem, however, a complete understanding of the mechanisms of the critical heat flux condition is not yet obtained.

For uniformly heated tubes in which a liquid is vaporized, the critical heat flux condition occurs first at the exit end of the tube. It has been noted that the mechanism of the critical condition varies according to the exit vapor quality. The mechanisms usually considered are DNB (departure from nucleate boiling) for a region of low exit qualities and dryout for a region of high exit qualities [1]. However, there is uncertainty as to the boundary between the two regions, and also it may be possible to consider several mechanisms that lead to the occurrence of the critical condition in the high quality annular flow region.

By making measurements of the film flow rate of a climbing liquid film on a heated rod, Hewitt *et al.* [2] demonstrated that the critical condition occurred when the film flow rate decreased smoothly to zero. This concept was confirmed by the succeeding work of Hewitt *et al.* [3, 4] for the usual forced flow boiling systems of a subcooled liquid at the tube inlet over a range of heat fluxes. Whalley, Hutchinson and Hewitt [5] proposed a method for calculating the critical heat flux taking into account droplet interchange between the annular liquid film and the vapor core along the tube length. In this method, the critical condition was assumed to occur when the liquid film flow rate at the exit end fell to zero. Ueda, Tanaka and Koizumi [6] made measurements of R-113 high quality flow in a uniformly heated tube with relatively low heat fluxes, and showed that the location of a sharp rise in wall temperature coincided well with the location predicted the liquid film flow rate to be zero.

However, it seems to be possible to assume another mechanisms of the critical condition than the liquid film dryout mentioned above, in the case of high heat fluxes where intensive nucleate boiling takes place under the liquid film. Todreas and Rohsenow [7] suggested the critical condition by nucleation-induced disruption of the annular liquid film, in connection with the upstream critical condition for non-uniform axial heat flux distributions. Ueda and Kim [8] measured the critical heat flux and the liquid film flow rate at the exit end of the heating section with R-113 upward flow in a uniformly heated tube of 10 mm I.D. and 2.45 m long. The result showed that the exit film flow rate at the critical condition was near to zero for low heat fluxes, however, it revealed a trend to increase with increasing critical heat flux over a certain value. This trend has been found, although not so clear, in the data of AERE Harwell [9] and also in the data of Staniforth and Stevens [10] obtained with R-12 upflow.

Ueda, Inoue and Nagatome [11] investigated the critical heat flux and the exit film flow rate with boiling liquid films falling down on outside surface of a vertical tube heated uniformly, and divided the characteristics of the critical heat flux into three types according to the exit film flow rate as follows:

Type I: The sharp rise in wall temperature occurs due to a reduction of the exit film flow rate to an extremely low value.

Type II: The boiling film is distorted and critical condition takes place by film disruption, i.e. by forming a stable dry patch in a thinned film area near the exit end.

Type III: The critical condition seems to be associated with main film separation resulting from high vapor generation on the heated surface.

Then, the present study was undertaken to examine the relationship between the critical heat flux and the exit film flow rate for a forced flow boiling system with high heat fluxes. With a view to attaining an insight into the mechanism, the characteristics of the critical heat flux were discussed comparing with those appeared in boiling of falling films. Measurements were made with a uniformly heated tube in which R-113 was vaporized from subcooled liquid at the inlet to a relatively high quality at the exit.

2. APPARATUS AND PROCEDURE

A flow diagram of the apparatus is shown in Fig. 1. The test section arranged vertically is a stainless-steel tube of 10.0 mm I.D., 12 mm O.D., and the heating section is 1.50 m in length. Fluorocarbon R-113 liquid in a storage tank was supplied by a circulating pump to the test tube through a preheater, and flowed upwards in the test tube. The test tube was heated uniformly by passing an alternating current through it, and the axial temperature distribution was measured with thirty-two thermocouples fitted along the tube length.

At the exit end of the test tube, a part of the liquid flows as an annular film on the wall surface and the remaining liquid is entrained in the vapor flow as droplets. For measuring the liquid film flow rate at the exit end, a method was used to extract the liquid film through a porous sintered tube of 10 mm I.D. and 70 mm long provided in the upper tube. For reference, the other method to remove the liquid film through a gap provided between the exit of the heated tube and the inlet of the upper tube, which was the same one used by Ueda and Kim [8], was also applied for some mass flow rate conditions in case of $x_{in} = -0.178$.

The exit film flow rate decreased with increasing power input to the heating section. The power input was increased in small steps keeping the inlet liquid subcool and the liquid flow rate at a set of values, until a sharp rise in wall temperature was observed at the exit end of the heating section. At each power level, measurements were made of the wall temperatures and the exit film flow rate. Figure 2 shows variations of heat transfer coefficient with quality obtained at heat fluxes a little higher than the critical condition at the exit end of the heating section. The heat transfer coefficient was derived by

$$h_{TP} = q/(T_w - T_b) \tag{1}$$

where, T_w is the inner surface temperature calculated from the measured outer surface temperature, and T_b is the mean bulk fluid temperature which was assumed to be T_s in the saturated region. The inlet pressure of the test tube was maintained at a value $p_{in} = 3.2 \times 10^5$ Pa through this experiment. The experimental ranges covered are

Mass velocity	$G = 350 \sim 1700\ \mathrm{kg\,m^{-2}\,s^{-1}}$
Heat flux	$q = (0.4 \sim 1.8) \times 10^5\ \mathrm{W\,m^{-2}}$
Inlet quality	$x_{in} = -0.178$ and -0.325.

3. CRITICAL HEAT FLUX AND EXIT QUALITY

The power input to the heating section was increased step by step under constant inlet conditions, and the critical heat flux q_c—the heat flux just before the sharp rise in wall temperature—was measured. Figure 3 shows the critical heat flux plotted against the exit quality calculated by

$$x_{exc} = x_{in} + \frac{4Lq_c}{GDh_{fg}}. \tag{2}$$

The solid plots in this figure are the data of Ueda and Kim [8] obtained with a heating section of $L = 2.45$ m.

In the scope of the present experiment, the heat transfer in a high quality region revealed, as is shown in Fig. 2, the characteristics in forced convection evaporation, i.e. a trend to increase the heat transfer coefficient with increasing quality. Therefore, the flow pattern in the downstream part of the tube was estimated to be annular type.

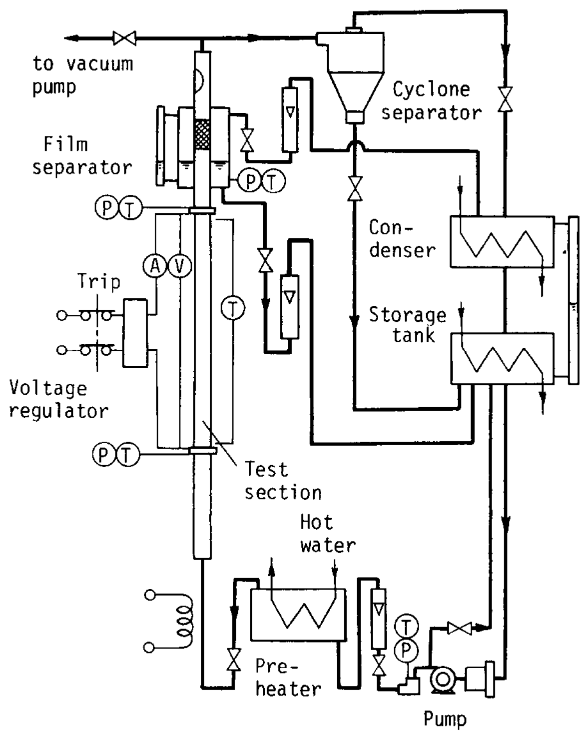

FIG. 1. Schematic diagram of experimental apparatus.

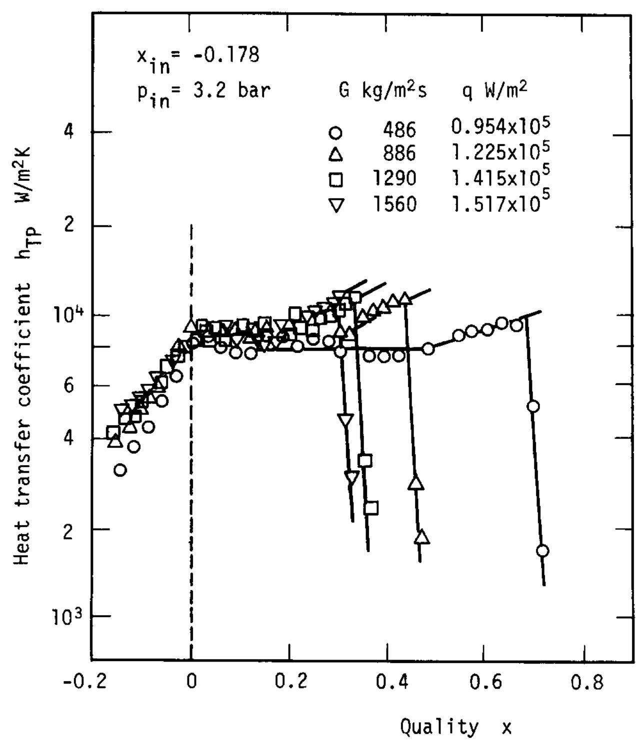

FIG. 2. Variation of heat transfer coefficient along tube length.

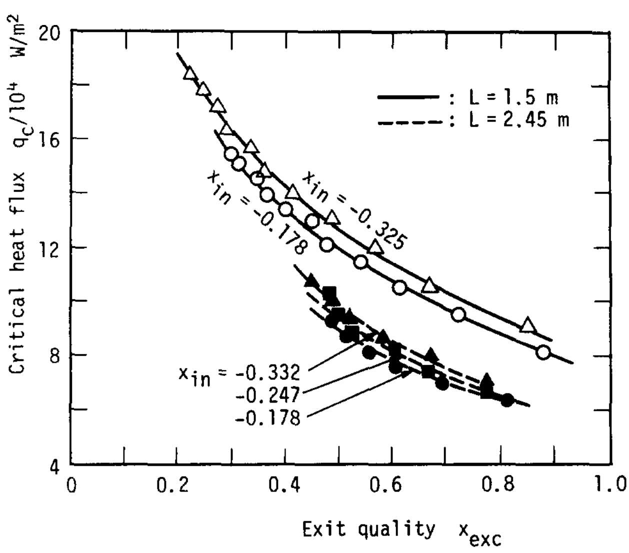

FIG. 3. Relation between critical heat flux and exit quality.

Figure 4 represents a flow pattern map derived from the Baker chart [12] for R-113 at 2.75 × 10^5 Pa, a mean pressure at the exit of the tube in this experiment. The open symbols plotted in this figure indicate the exit qualities at the critical condition. This figure is also suggesting the flow pattern near the exit end to be annular or annular-dispersed flow, even in case of high mass velocities and relatively low exit qualities. The solid plot shows the quality at the location where the heat transfer coefficient changes its characteristics from nucleate boiling of a near constant value to forced convection evaporation (Fig. 2).

Katto [13–16] has investigated the critical heat flux data for force flow boiling in uniformly heated tubes, and proposed generalized correlations dividing the critical heat flux into four characteristic regimes, called *L*-, *H*-, *N*- and *HP*-regimes. Figure 5 illustrates comparison of the present data with the Katto's correlations for the basic critical heat flux. The numerals attached to the data points indicate the value of L_s/D, where L_s is the boiling length, i.e. the tube length from the location of $x = 0$ to the exit end of the heating section. Most of the present data are ranged in the *H*-regime, excepting the data for the lowest mass velocity which are belonging to the *L*-regime. The present result shows a little lower values, however, is in good agreement with the correlations in a trend.

4. LIQUID FILM FLOW RATE AT EXIT END OF HEATING SECTION

For measuring the exit film flow rate, a method with a porous sintered tube was used to extract the liquid. In this method [17], some amount of vapor were extracted with the liquid. The liquid extraction rate increased rapidly at first and then tended to level off with increasing vapor extraction rate. The level of the plateau in the curve was considered as the liquid film flow rate at there.

The liquid film flow rate at the exit end of the heating section was obtained by subtracting the droplet deposition rate in the unheated tube of 264 mm long, installed between the exit end and the sintered tube, from the measured film flow rate. The variation of the film flow rate along the unheated tube is expressed by

$$\frac{dM_f}{dz} = \pi DKC \tag{3}$$

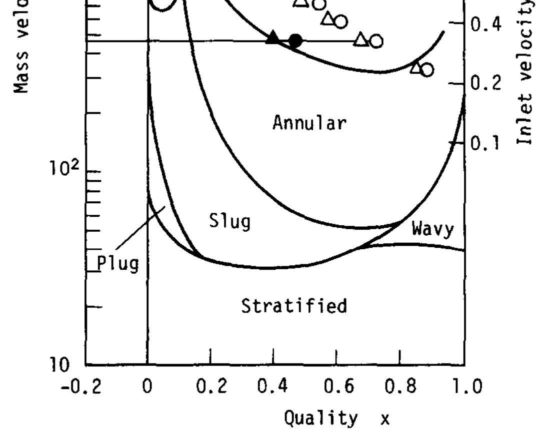

FIG. 4. Flow pattern map.

where K is the droplet deposition coefficient and C is the mean droplet concentration in the vapor core. The value of K was evaluated from an empirical equation of Ueda, Tanaka and Koizumi [6]—equation (14) in the paper—derived for K under similar experimental conditions of R-113 to the present test. The deposition rate thus calculated for the unheated length ranged from 0.5 to 3.0 kg h^{-1}. A correction was also made, though it was a small value, of the extracted liquid evaporation due to a pressure drop through the sintered tube.

Figure 6 shows the results of the exit film flow rate obtained for the inlet qualities $x_{in} = -0.178$ and -0.325. The exit film flow rate decreased steadily as the heat flux was increased. A solid symbol plotted at the end of each curve represents the exit film flow rate at the critical condition. The points of symbol $\times$ in the figure for $x_{in} = -0.178$ indicate the data at the critical condition measured with a gap device instead of the sintered tube. The present results show clearly that the exit film flow rate at the critical condition increases, as with the result of Ueda and Kim [8], with increasing heat flux when the heat flux is higher than about 10^5 W m^{-2}.

Figure 7 represents the relationship between the critical heat flux and the exit film flow rate per unit periphery at the critical condition

$$\Gamma_{exc} = M_{fexc}/\pi D.$$

Figure 8 shows the exit quality at the critical condition plotted against the exit film flow rate Γ_{exc}. The open symbols in these figures are the data of the present experiment and the solid symbols are those obtained by Ueda and Kim. Both data indicate that the exit film flow rate at the critical condition is near to zero less than about 0.05 kg m^{-1} s^{-1} in all cases of the exit qualities higher than 50%, however, the exit film flow rate increases steeply as the heat flux is increased and the exit quality decreases less than 50%.

5. CORRELATION OF THE CRITICAL CONDITION

Behavior of the liquid film seems to be complicated at the critical condition. Then, the relation between the critical heat flux and the exit film flow rate was discussed by comparing with those appeared in boiling of falling liquid films [11]. For this purpose, the thickness and mean velocity of the liquid film were estimated. The liquid film flow rate per unit periphery is expressed as

$$\Gamma = \mu_l \int_0^{y_i^+} u^+ \, dy^+ \tag{4}$$

where

$$u^+ = u \Big/ \left(\frac{\tau_w}{\rho_l}\right)^{0.5}, \quad y^+ = \frac{y}{\nu_l}\left(\frac{\tau_w}{\rho_l}\right)^{0.5}.$$

Here, the assumptions are used for simplification that no vapor bubble is involved in the liquid film and that the velocity distribution in the film can be approximated by the Karman's universal velocity profile. Then, the liquid film flow rate Γ can be expressed in terms of the non-dimensional film thickness.

$$y_i^+ = \frac{y_i}{\nu_l}\left(\frac{\tau_w}{\rho_l}\right)^{0.5}. \tag{5}$$

Therefore, the film thickness at the exit end y_{iex} can be

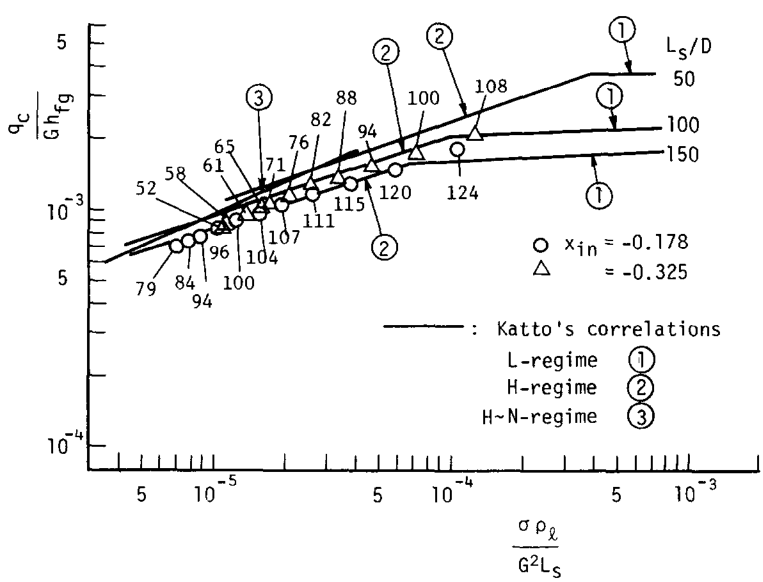

FIG. 5. Critical heat flux (Comparison with Katto's correlations).

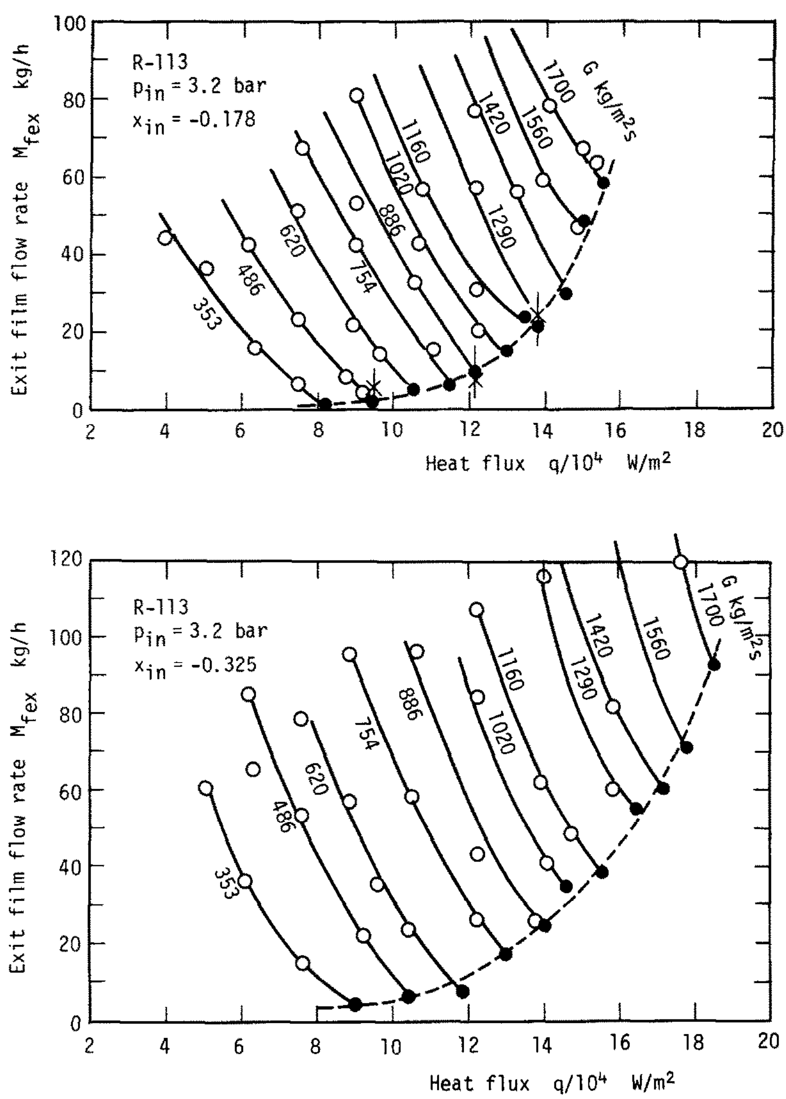

FIG. 6. Variation of exit film flow rate with heat flux.

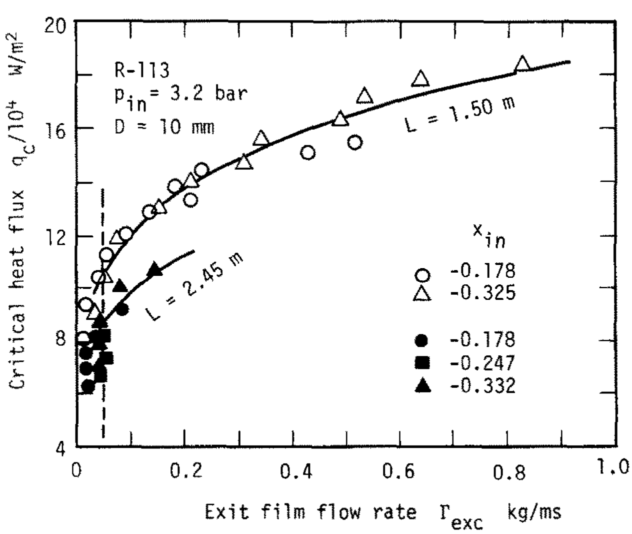

FIG. 7. Relation between critical heat flux and exit film flow rate.

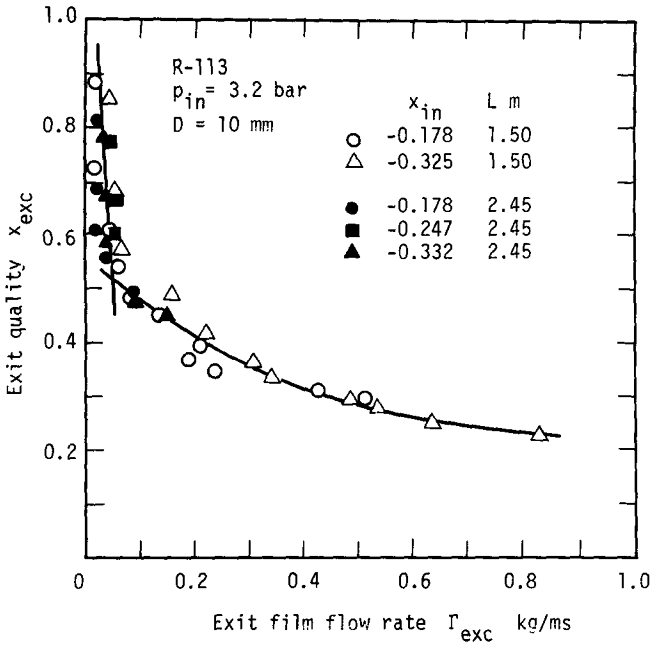

FIG. 8. Exit film flow rate at critical heat flux condition.

derived from the measured film flow rate Γ_{ex} by applying the wall shear stress τ_w into this equation, and the mean film velocity is found by

$$u_m = \Gamma_{ex}/\rho_l\, y_{iex}. \tag{6}$$

The Lockhart–Martinelli correlation [18] was used for predicting the wall shear stress. The wall shear stress is expressed in terms of the frictional pressure drop gradient as

$$\tau_w = \frac{D}{4}\left(\frac{dp}{dz}\right)_F = \frac{D}{4}\left(\frac{dp}{dz}\right)_G \Phi_G^2$$

where $(dp/dz)_G$ is the single-phase pressure gradient for the vapor phase flowing alone in the tube

$$\left(\frac{dp}{dz}\right)_G = \frac{2f_G G_G^2}{D\rho_g}.$$

By applying Colburn's equation to the friction factor f_G and substituting $G_G = Gx_{ex}$, the wall shear stress can be rearranged to give

$$\tau_w = 0.023\left(\frac{GD}{\mu_g}\right)^{-0.20}\frac{G^2}{\rho_g}x_{ex}^{1.8}\,\Phi_G^2 \tag{7}$$

where Φ_G is a function of a parameter

$$X_{tt} = \left(\frac{1-x_{ex}}{x_{ex}}\right)^{0.9}\left(\frac{\rho_g}{\rho_l}\right)^{0.5}\left(\frac{\mu_l}{\mu_g}\right)^{0.1} \tag{8}$$

and may be expressed approximately by the following equation [19]

$$\Phi_G = 1 + 2.85\,X_{tt}^{0.523}. \tag{9}$$

Then, an attempt was made to correlate the critical condition with the film thickness y_{ic} and the mean velocity u_{mc} thus derived for the measured exit film flow rate at the critical condition Γ_{exc}.

For the limiting condition of liquid film disruption by formation of stable dry patches, the following parameter expressing the ratio of the dynamic force of film flow to the surface tension

$$\rho_l u_{mc}^2\, y_{ic}/\sigma$$

seems to be connected with. Figure 9 shows the ratio of evaporation rate to exit film flow rate, $(q_c/h_{fg})/\rho_l u_{mc}$, for the data presented in Fig. 8, which is plotted against the above parameter in a similar manner to the correlation of falling films. Comparison with the characteristics of the critical heat flux in falling film boiling indicates that the boundary of type I is corresponding to an extremely low flow rate, and that the present result is quite different from the characteristics of type II, i.e. the film disruption caused by boiling film distortion. The present result shows a trend which would be obtained when the liquid film is less distorted around the tube periphery. This is presumably ascribed to the fact that the liquid film in the forced flow boiling is driven by a vapor stream of high velocity and possesses a high momentum. The film velocity of the present data was about five times as high as that in the falling film boiling.

When the exit quality is higher than 50%, as shown in Fig. 8, the exit film flow rate Γ_{exc} is less than about 0.05 kg m^{-1} s^{-1} This flow rate is small enough and is comparable order with the errors which may result from the methods for measuring the critical heat flux and the liquid film flow rate in this experiment. Therefore, the critical condition in this range of the present experiment is thought to occur, as mentioned

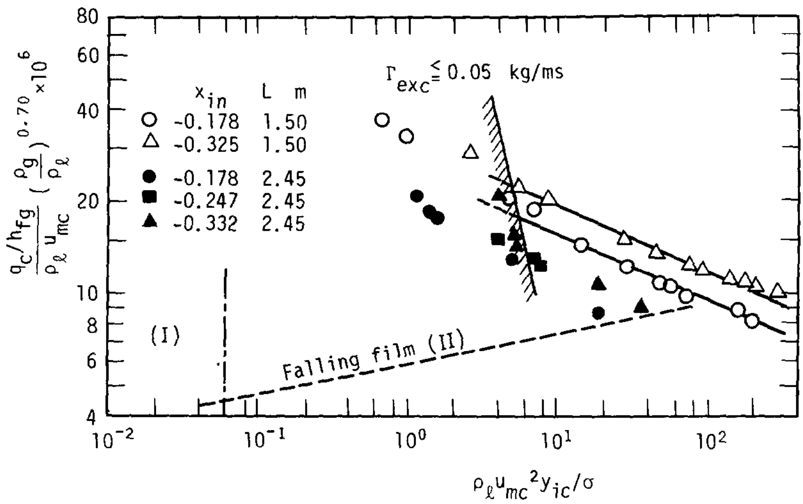

FIG. 9. Correlation of critical heat flux.

by Hewitt *et al.* [2–4], by a reduction of the liquid film flow rate at the exit end to some near zero value. However, the exit film flow rate at the critical condition increases steeply as the heat flux is increased and the exit quality decreases less than 50%. Then, the critical heat flux data of the exit film flow rate Γ_{exc} greater than 0.05 kg m^{-1} s^{-1} were plotted, in the same way as the type III in falling film boiling, against the Weber number

$$We = \rho_l u_{mc}^2 L_s/\sigma$$

where L_s is the boiling length. Since the inlet liquid was subcooled in the present systems, the boiling length was used instead of the heating length L.

Figure 10 shows the result, indicating that the critical condition data in forced flow boiling with high heat fluxes are well correlated by the Weber number defined for the exit film velocity u_{mc}. The value $(\rho_g/\rho_l)^{0.08}$ at the exit condition of the present test is 0.708. Then, the result can be expressed as

$$\frac{q_c/h_{fg}}{\rho_l u_{mc}} = 0.042\left(\frac{\rho_l u_{mc}^2 L_s}{\sigma}\right)^{-0.38}. \quad (10)$$

The values of this equation are about 2.5 times as high as those of the equation correlating the type III in falling film boiling, however, the gradient of both equations for the Weber number is in fairly good agreement. In the forced flow boiling, it has been noted that an amount of heat is transferred by convection in the annular liquid film and subsequent evaporation at the interface, and the vapor generation by bubble nucleation on the heated surface is relatively limited. Therefore, it looks like reasonable that the heat flux required to reach a state of high bubble nucleation on the surface in the forced flow boiling is higher than that in the falling film boiling. Then, it seems to be that, as with the case of type III in falling film boiling, the main film separation from the heated surface by bubble nucleation takes an important role of the critical phenomenon in forced flow boiling with high heat fluxes.

6. CONCLUSIONS

As a result of the experimental investigation on the critical heat flux and the exit film flow rate of R-113 forced flow boiling in a uniformly heated tube, the following conclusions are obtained

(1) The liquid film flow rate at the exit end of the heating section decreases progressively with increasing heat flux. In a range of relatively low heat fluxes and high exit qualities, the critical condition occurs when the exit film flow rate decreases to some near zero value.

(2) In a range of high heat fluxes, however, the exit film flow rate at the critical condition increases as the heat flux is increased and the exit quality decreases less than 50%.

(3) The critical heat flux condition data in the range of high heat fluxes are correlated by equation (10). Comparing the characteristics with those of falling film boiling, it appears to be that the liquid film separation from the heated surface by vapor generation is closely related to the occurrence of the critical condition.

Acknowledgements—The authors gratefully acknowledge the support for this work by the research fund (Grant in Aid of Energy Special Project Research, 1979 and 1980) of the Ministry of Education, Japan.

REFERENCES

1. J. G. Collier, *Convective Boiling and Condensation*, pp. 129–135 and 285–292, McGraw-Hill, London (1972).
2. G. F. Hewitt, H. A. Kearsey, P. M. C. Lacey and D. J. Pulling, Burnout and nucleation in climbing film flow, *Int. J. Heat Mass Transfer* **8**, 793–814 (1965).
3. G. F. Hewitt, H. A. Kearsey, P. M. C. Lacey and D. J.

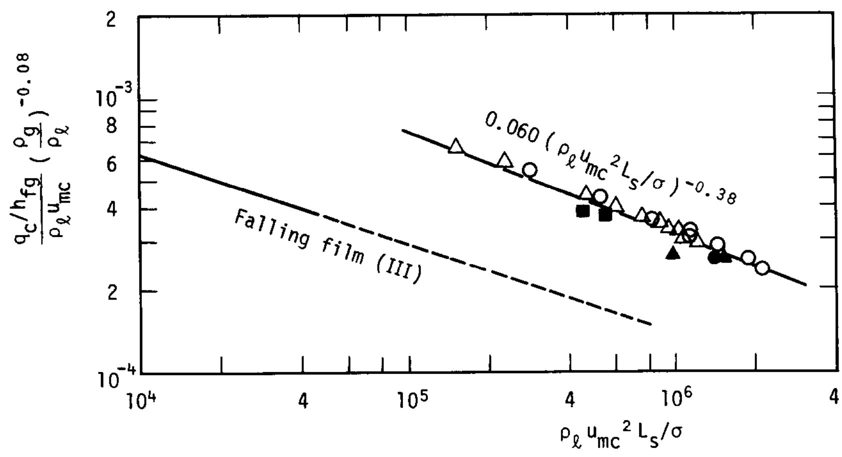

FIG. 10. Correlation of critical heat flux. Keys are given in Fig. 9.

Pulling, Burn-out and film flow in the evaporation of water in tubes, *Proc. Instn mech. Engrs* **180**, 206–215 (1966).
4. A. W. Bennett, G. F. Hewitt, H. A. Kearsey, R. K. F. Keeys and D. J. Pulling, Studies of burnout in boiling heat transfer. *Trans. Instn chem. Engrs* **45**, T319–T333 (1967).
5. P. B. Whalley, P. Hutchinson and G. F. Hewitt, The calculation of critical heat flux in forced convection boiling, *Proc. 5th Int. Heat Transfer Conf., Tokyo* **4**, 290–294 (1974).
6. T. Ueda, H. Tanaka and Y. Koizumi, Dryout of liquid film in high quality R-113 upflow in a heated tube, *Proc. 6th Int. Heat Transfer Conf., Toronto* **1**, 423–428 (1978).
7. N. E. Todreas and W. M. Rohsenow, The effect of axial heat flux distribution on critical heat flux, *Proc. 3rd Int. Heat Transfer Conf., Chicago* **3**, 78–85 (1966).
8. T. Ueda and K. K. Kim, Dryout heat flux and size of entrained drops in a flow boiling system, *Preprint of 16th Japan Heat Transfer Symp.*, 211–213 (1979).
9. G. F. Hewitt and N. S. Hall-Taylor, *Annular Two-phase Flow*, pp. 225–227. Pergamon Press (1970).
10. R. Staniforth and G. F. Stevens, Experimental studies of burn-out using Freon 12 at low pressure, with reference to burn-out in water at high pressure. *Proc. Instn mech Engrs* **180**, 216–225 (1966).
11. T. Ueda, M. Inoue and S. Nagatome, Critical heat flux and droplet entrainment rate in boiling of falling liquid films, *Int. J. Heat Mass Transfer* **24**, 1257–1266 (1981).
12. O. Baker, Simultaneous flow of oil and gas, *Oil Gas J.* **53**, 185–190 (1954).
13. Y. Katto, A generalized correlation of critical heat flux for the forced convection boiling in vertical uniformly heated round tubes, *Int. J. Heat Mass Transfer* **21**, 1527–1542 (1978).
14. Y. Katto, An analysis of the effect of inlet subcooling on critical heat flux of forced convection boiling in vertical uniformly heated tubes, *Int. J. Heat Mass Transfer* **22**, 1567–1575 (1979).
15. Y. Katto, General features of CHF of forced convection boiling in uniformly heated vertical tubes with zero inlet subcooling, *Int. J. Heat Mass Transfer* **23**, 493–504 (1980).
16. Y. Katto, Critical heat flux of forced convection boiling in uniformly heated vertical tubes (Correlation of CHF in HP-regime and determination of CHF-regime map), *Int. J. Heat Mass Transfer* **3**, 1573–1580 (1980).
17. E. O. Moeck, Measurement of liquid film flow and wall shear stress in two-phase flow, *11th Nat. ASME/AIChE Heat Transfer Conf., Two-phase Flow Instrumentation*, 36–46 (1969).
18. R. W. Lockhart and R. C. Martinelli, Proposed correlation of data for isothermal two-phase, two-component flow in pipes, *Chem. Engng Prog.* **45**, 39–48 (1949).
19. M. Soliman, J. R. Schuster and P. J. Berenson, A general heat transfer correlation for annular flow condensation, *Trans. ASME* **90C** 267–276 (1968).

FLUX DE CHALEUR CRITIQUE ET DEBIT DE SORTIE DU FILM DANS UN SYSTEME EN EBULLITION

Résumé—On mesure le flux de chaleur critique et le débit de sortie du film liquide à l'extrémité d'un tube avec du Fréon-113 en écoulement ascendant dans un tube chauffé uniformément. Le débit de sortie du film dans la condition de flux critique est proche de zéro dans tous les cas où la qualité est supérieure à 50% en sortie, mais le débit de sortie du film croît lorsque le flux est augmenté et la qualité à la sortie est inférieure à 50%. Une formule est proposée pour la condition critique avec des flux thermiques élevés ; elle suggère que la séparation du film liquide de la surface chaude par la création de vapeur prend une place importante dans le phénomène critique.

KRITISCHE WÄRMESTROMDICHTE UND AUSTRITTS-FILMMASSENSTROM BEIM STRÖMUNGSSIEDEN

Zusammenfassung—Die kritische Wärmestromdichte und der Massenstrom des Flüssigkeitsfilms am Austritt des Versuchsrohrs wurden bei aufwärts gerichteter Strömung von R-113 bei gleichförmiger Beheizung gemessen. Bei der kritischen Wärmestromdichte ist der Austritts-Filmmassenstrom bei Austritts-Dampfmassenanteilen $>50\%$ in allen Fällen nahe null; er nimmt jedoch zu, wenn die Wärmestromdichte erhöht wird und der Austritts-Dampfmassenanteil 50% unterschreitet. Für die kritische Bedingung bei hohen Wärmestromdichten wird eine Korrelation vorgeschlagen, die auf der Annahme beruht, daß die Abtrennung des Flüssigkeitsfilms von der Heizfläche durch Dampfbildung von maßgeblichem Einfluß ist.

КРИТИЧЕСКИЙ ТЕПЛОВОЙ ПОТОК И СКОРОСТЬ ТЕЧЕНИЯ ПЛЕНКИ НА ВЫХОДНОМ УЧАСТКЕ ТРУБЫ ПРИ ПЛЕНОЧНОМ КИПЕНИИ

Аннотация — Измерены величина критического теплового потока и скорость течения жидкой пленки на выходном участке равномерно нагреваемой трубы при восходящем течении фреона-113. В условиях критического теплового потока скорость течения пленки на выходе равнялась примерно нулю во всех случаях, когда паросодержание превышало 50%, однако она возрастала по мере того, как происходило увеличение теплового потока при паросодержании на выходном участке трубы менее 50%. Установлена корреляция высоких значений тепловых потоков и условия возникновения кризиса кипения в предположении, что важную роль в этом явлении играет оттеснение пленки жидкости от нагреваемой поверхности образующимся паром.